Critical Behavior of a Strongly Interacting 2D Electron System

A. Mokashi,[1] S. Li,[2] B. Wen,[2] S. V. Kravchenko,[1] A. A. Shashkin,[3] V. T. Dolgopolov,[3] and M. P. Sarachik[2]

[1]*Physics Department, Northeastern University, Boston, Massachusetts 02115, USA*

[2]*Physics Department, City College of the City University of New York, New York, New York 10031, USA*

[3]*Institute of Solid State Physics, Chernogolovka, Moscow District 142432, Russia*

(Received 19 June 2012; published 28 August 2012)

With decreasing density n_s the thermopower S of a low-disorder two-dimensional electron system in silicon is found to exhibit a sharp increase by more than an order of magnitude tending to a divergence at a finite disorder-independent density n_t consistent with the critical form $(-T/S) \propto (n_s - n_t)^x$ with $x = 1.0 \pm 0.1$ (T is the temperature). Our results provide clear evidence for an interaction-induced transition to a new phase at low density in a strongly interacting 2D electron system.

DOI: 10.1103/PhysRevLett.109.096405 PACS numbers: 71.30.+h, 71.18.+y, 73.40.Qv

The behavior of strongly interacting electrons in two dimensions is a forefront area of condensed matter physics in which theoretical methods are still poorly developed and new experimental results are of great interest. Consistent with Fermi liquid theory at high electron densities [1], these two-dimensional (2D) systems are expected to undergo one or more transitions to spatially and/or spin-ordered phases as the density is decreased, ultimately forming a Wigner crystal in the dilute, strongly interacting limit [2–6]. The interaction strength is characterized by the ratio of the Coulomb energy to the Fermi energy, determined by the dimensionless parameter $r_s = 1/(\pi n_s a_B^2)^{1/2}$ (here n_s is the areal density of electrons, $a_B = \varepsilon\hbar^2/m_b e^2$, and ε, e, and m_b are the dielectric constant, the absolute value of the electron charge, and the band mass, respectively); the parameter r_s is proportional to $n_s^{-1/2}$ and increases with decreasing electron density, reaching values in excess of $r_s \gtrsim 10$ in systems investigated experimentally to date. Particularly strong many-body effects have been observed in silicon metal-oxide-semiconductor field-effect transistors.

In this Letter we report that the thermopower of a low-disorder 2D electron system in silicon exhibits critical behavior with decreasing electron density, tending toward a divergence at a well-defined disorder-independent density n_t. Our results provide clear evidence for an interaction-induced transition to a new phase at low density which may be a precursor phase, or a direct transition to the long sought-after Wigner solid.

The thermopower is defined as the ratio of the thermoelectric voltage to the temperature difference, $S = -\Delta V/\Delta T$. Measurements were made in a sample-in-vacuum Oxford dilution refrigerator with a base temperature of ≈ 30 mK on (100)-silicon metal-oxide-semiconductor field-effect transistors similar to those previously used in Ref. [7]. The advantage of these samples is a very low contact resistance (in ''conventional'' silicon samples, high contact resistance becomes the main experimental obstacle in the low-density low-temperature limit). To minimize the contact resistance, thin gaps in the gate metallization have been introduced, which allows for maintaining a high electron density near the contacts regardless of its value in the main part of the sample. The electron density was controlled by applying a positive dc voltage to the gate relative to the contacts; the oxide thickness was 150 nm. Samples were used with a Hall bar geometry of width 50 μm and distance 120 μm between the central potential probes, and measurements of the thermoelectric voltage were obtained in the main part of the sample [shaded in the inset to Fig. 1(a)]. A Hall contact pair, either 1-5 or 4-8, was employed as a heater: the 2D electrons were locally heated by passing an ac current at a low frequency f through either pair. Both the source and drain contacts were thermally anchored. In such an arrangement it was possible to reverse the direction of the temperature gradient induced in the central region of the sample. The temperatures of the central probes were determined using two thermometers glued to the metallic pads on the sample holder connected by metallic wires to the contacts on the sample; the temperature gradients between the contacts reached 1–5 mK over the distance. The measured temperatures were independent of the electron density in the central region, indicating that the heat flowed from the heater to the anchor through the lattice, so that our experiment is similar to a standard setup for thermopower measurements. The average temperature determined by the thermometers was checked to correspond to the average electron temperature in the central region measured using the calibrated sample resistivity. The temperature difference between the pairs of contacts 6, 7, and the source or drain along the thermal path from the heater to the anchor was monitored and found to be proportional to the distance between the contacts, as expected. Constantan or superconducting wiring was employed to minimize heat leaks from the sample. Possible rf pickup was carefully suppressed, and the thermoelectric voltage was measured using a low-noise low-offset LI-75A preamplifier and a lock-in amplifier in the $2f$ mode in the

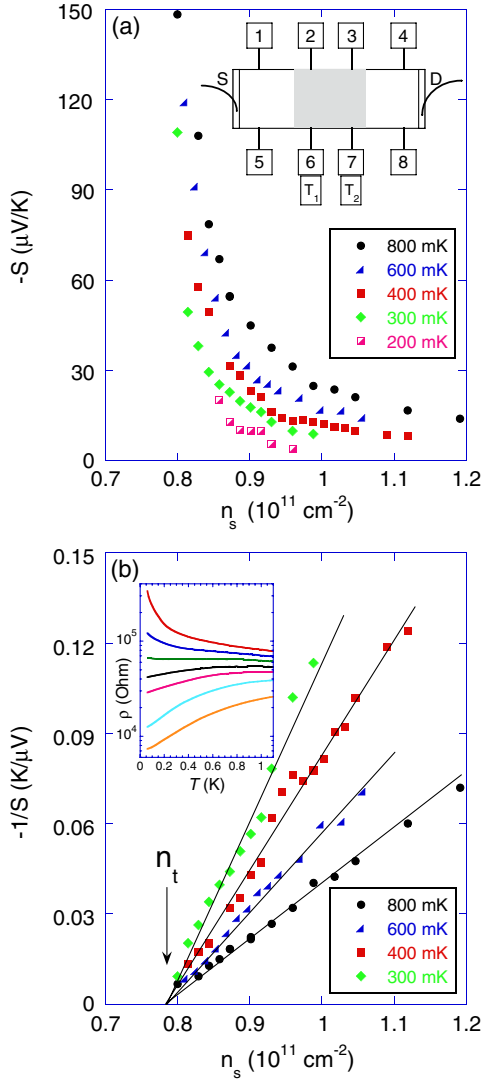

FIG. 1 (color online). (a) Thermoelectric power, S, as a function of electron density n_s at different temperatures. Many data points are omitted for clarity. The inset is a schematic view of the sample. The contacts include four pairs of potential probes, source, and drain; the main part of the sample is shaded. The thermometers T_1 and T_2 measure the temperature of the contacts. (b) The inverse thermopower as a function of electron density at different temperatures. The solid lines denote linear fits to the data and extrapolate to zero at a density n_t. The inset shows the resistivity as a function of temperature for electron densities (top to bottom): 0.768, 0.783, 0.798, 0.813, 0.828, 0.870, and 0.914×10^{11} cm^{-2}.

frequency range 0.01–0.1 Hz. The sample resistance was measured by a standard four-terminal technique at a frequency 0.4 Hz. Excitation currents were kept sufficiently small (0.1–1 nA) to ensure that measurements were taken in the linear regime. The results shown in this Letter were obtained on a sample with a peak electron mobility close to 3 m^2/V s at $T = 0.1$ K.

Our experimental results are shown in Figs. 1–3. Figure 1(a) shows data for the thermopower as a function

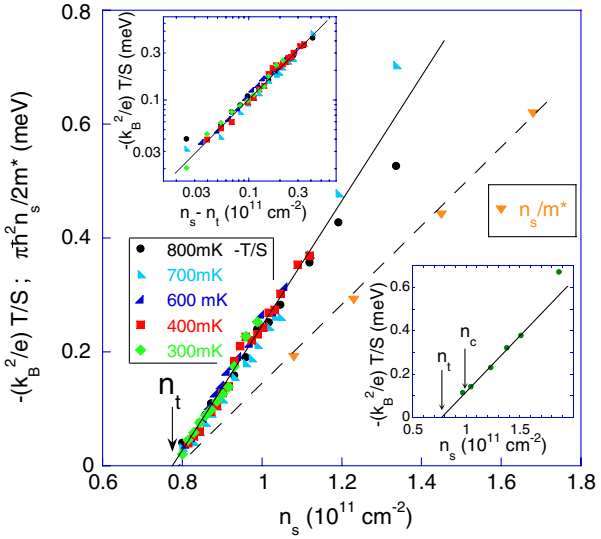

FIG. 2 (color online). $(-T/S)$ versus electron density n_s for different temperatures. The solid line is a linear fit which extrapolates to zero at n_t. Also shown is the effective mass m^* obtained for the same samples by different measurements [10]. The dashed line is a linear fit. Inset, upper left-hand corner: log-log plot of $(-T/S)$ versus $(n_s$-$n_t)$, demonstrating power law approach to the critical density n_t. Inset, lower right-hand corner: $(-T/S)$ versus density at $T = 0.3$ K for a highly-disordered 2D electron system in silicon [8]. The linear fit (solid line) extrapolates to zero at the same density n_t. The position of the density n_c for the metal-insulator transition was estimated to be $0.99 \pm 0.02 \times 10^{11}$ cm^{-2}.

of n_s at different temperatures. $(-S)$ increases strongly with decreasing electron density and becomes larger as the temperature is increased. The divergent behavior of the thermopower is evident when plotted as the inverse quantity $(-1/S)$ versus electron density in Fig. 1(b).

Figure 2 shows $(-T/S)$ plotted as a function of n_s. The data collapse onto a single curve demonstrating that the thermopower S is a linear function of temperature. In turn, the ratio $(-T/S)$ is a function of electron density n_s of the form

$$(-T/S) \propto (n_s - n_t)^x. \quad (1)$$

Fits to this expression indicate that the thermopower diverges with decreasing electron density with a critical exponent $x = 1.0 \pm 0.1$ at a density $n_t = 7.8 \pm 0.1 \times 10^{10}$ cm^{-2} that is close to (or the same as) the density for the metal-insulator transition $n_c \approx 8 \times 10^{10}$ cm^{-2}, obtained from resistivity measurements in this low-disorder electron system [see the inset to Fig. 1(b)]. The log-log plot shown in the inset (upper left-hand corner) of Fig. 2 demonstrates the critical, power law behavior of the thermopower.

In Fig. 3 we show the product $(-S\sigma)$ that determines the thermoelectric current $j = -S\sigma\nabla T$ as a function of electron density at two different temperatures (here σ is the

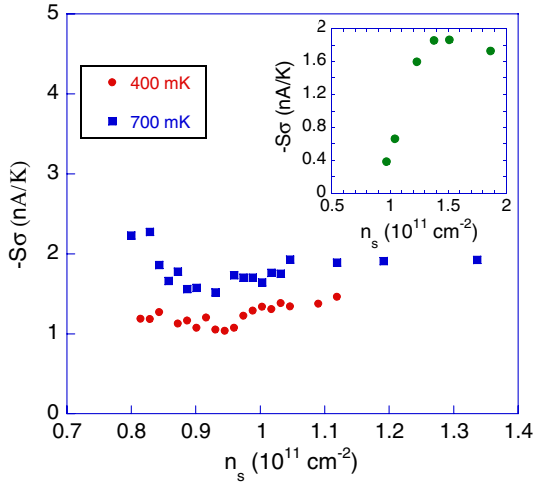

FIG. 3 (color online). The product $(-S\sigma)$ that determines the thermoelectric current plotted as a function of electron density n_s at different temperatures. Inset: $(-S\sigma)$ versus electron density at $T = 0.3$ K for a highly-disordered 2D electron system in silicon [8]. The density n_c for the metal-insulator transition in this high-disorder sample is shown in the lower right-hand inset of Fig. 2.

conductivity). $(-S\sigma)$ is approximately constant in the critical region; i.e., $(1/S)$ is proportional to σ in the low-disorder 2D electron system. Within the relaxation time approximation, one expects the thermopower S to depend only weakly on scattering, while the scattering should play a major role in determining the conductivity. That $(S\sigma)$ is constant signals that disorder is not the origin of the critical behavior in our samples, which derives instead from strong electron-electron interactions. The fact that the behavior shown in Fig. 2 continues smoothly down to the lowest electron densities achieved confirms that the disorder effects that might cause deviations are minor.

Confirmation is provided by comparison with earlier data obtained by Fletcher *et al.* [8] in a silicon sample with a high level of disorder, as indicated by the appreciably higher density n_c for the resistively determined metal-insulator transition. A replot of the thermopower taken from Ref. [8], shown in the lower right-hand inset of Fig. 2, demonstrates that $(-T/S)$ measured well above the critical point extrapolates to the same density n_t. However, in contrast with our data, $(-S\sigma)$ for the higher-disorder silicon samples tends to zero at the higher-density transition point n_c (see inset to Fig. 3) due to a rapidly decreasing conductivity σ for $n_s < n_c$. Thus, while the resistive transition n_c varies with disorder, the divergence of the thermopower occurs at a density n_t that is independent of disorder [9]. This indicates clearly that the transitions in low- and high-disorder silicon derive from different sources: whereas in highly-disordered 2D electron systems the conductivity tends to zero due to disorder, in the clean 2D electron system the drop of the conductivity occurs at the transition driven by electron-electron interactions [10].

Based on Fermi liquid theory, Dolgopolov and Gold [11,12] recently obtained the following expression for the diffusion thermopower of strongly interacting 2D electrons in the low-temperature regime:

$$S = -\alpha \frac{2\pi k_B^2 m T}{3e\hbar^2 n_s}, \tag{2}$$

where k_B is Boltzmann's constant and m is the effective mass. This expression, which resembles the well-known Mott relation for noninteracting electrons, was shown to hold for the strongly interacting case provided one includes the parameter α that depends on both the disorder [13–15] and interaction strength [11,12]. The dependence of α on the electron density is rather weak, and the main effect of electron-electron interactions is to suppress the thermopower S.

Note that we have found $S \propto T$, as expected for the diffusion thermopower. This indicates that the phonon drag contribution is small in the temperature range of our experiments, and our measurements yield the contribution of interest, namely, the diffusion thermopower.

The measured $(-T/S)$, shown in Fig. 2, decreases linearly with decreasing electron density, extrapolating to zero at n_t. According to Eq. (2), $(-T/S)$ is proportional to (n_s/m), indicating a strong increase of the mass by more than an order of magnitude. Our results thus imply a divergence of the electron mass at the density n_t: $m \propto n_s/(n_s - n_t)$—behavior that is typical in the vicinity of an interaction-induced phase transition.

It is interesting to compare these results with the effective mass m^* obtained earlier for the same samples, where m^* and the g factor were determined by combining measurements of the slope of the conductivity versus temperature with measurements of the parallel magnetic field B^* for full spin polarization [10]. As seen in Fig. 2, the two data sets display similar behavior. However, the thermopower data do not yield the absolute value of m because of uncertainty in the coefficient α in Eq. (2). The value of m can be extracted from the thermopower data by requiring that the two data sets in Fig. 2 correspond to the same value of mass in the range of electron densities where they overlap. Determined from the ratio of the slopes, this yields a coefficient $\alpha \approx 0.18$. The corresponding mass enhancement in the critical region reaches $m/m_b \approx 25$ at $n_s \approx 8.2 \times 10^{10}$ cm^{-2}, where the band mass $m_b = 0.19m_e$ and m_e is the free electron mass. The mass $m \approx 5m_e$ exceeds by far the values of the effective mass obtained from previous experiments on the 2D electron system in silicon as well as other 2D electron systems.

It is important to note that the current experiment includes data for electron densities that are much closer to the critical point than the earlier measurements, and reports a much larger enhancement of the effective mass for reasons explained below.

The Zeeman field B^* required to fully polarize the spins and the thermopower measurements both imply a large enhancement of the effective mass [16]. However, the two experiments measure different effective masses: the thermopower gives a measure of the mass at the Fermi level, while B^* measures the mass related to the bandwidth, which is the Fermi energy counted from the band bottom. In other words, while the thermopower as well as the conductivity are sensitive to the low energy excitations within an energy range $\sim k_B T$ near the Fermi energy, the Zeeman field B^* for full spin polarization is a measure of the bandwidth and is sensitive to the behavior of all states including those relatively far from the Fermi energy.

For $n_s \geq 10^{11}$ cm^{-2}, the mass was found to be essentially the same [17,18], thereby justifying our determination of α. On the other hand, the behavior is different at the densities reached in our experiment in the very close vicinity of the critical point n_t ($n_s < 10^{11}$ cm^{-2}), where the bandwidth-related mass was found to increase by only a factor ≈ 4. Indeed, we argue that the bandwidth-related mass does not increase strongly near n_t. If so, the ratio of the spin and cyclotron splittings in perpendicular magnetic fields would increase considerably with decreasing electron density so that the spin-up and spin-down levels should cross whenever this ratio is an integer. One should then observe a Shubnikov–de Haas oscillation beating pattern with decreasing electron density, including several switches between the oscillation numbers in weak magnetic fields. Instead, the Shubnikov–de Haas oscillations in the dilute 2D electron system in silicon reveal one switch from cyclotron to spin minima (the ratio of the spin and cyclotron splittings reaches ≈ 1) as the electron density is decreased [19], the spin minima surviving down to $n_s \approx n_c$ and even below [20].

In effect, while the bandwidth does not decrease appreciably in the close vicinity of the critical point n_t and the effective mass obtained from such measurements does not exhibit a true divergence, the thermopower measurements yield the effective mass at the Fermi energy, which does indeed diverge.

A divergence of the effective mass has been predicted by a number of theories: by using Gutzwiller's theory [21], by using an analogy with He^3 near the onset of Wigner crystallization [22,23], by extending the Fermi liquid concept to the strongly interacting limit [24], by solving an extended Hubbard model using the dynamical mean-field theory [25], by using a renormalization group analysis for multivalley 2D systems [26], and by using Monte Carlo simulations [27,28]. Some theories predict that the disorder is important for the mass enhancement [26–28]. In contrast with most theories that assume a parabolic spectrum, the authors of Ref. [24] stress that there is a clear distinction between the mass at the Fermi level and the bandwidth-related mass. In this respect, our conclusions are consistent with the model of Ref. [24] in which a flattening at the Fermi energy in the spectrum leads to a diverging effective mass. This Fermi liquid-based model implies the existence of an intermediate phase that precedes Wigner crystallization.

There has been a great deal of debate concerning the origin of the interesting, enigmatic behavior in these strongly interacting 2D electron systems. In particular, many have questioned whether the change of the resistivity from metallic to insulating temperature dependence signals a phase transition, or whether it is a crossover. We close by noting that unlike the resistivity, which displays complex behavior that may not distinguish between these two scenarios, we have shown that the thermopower diverges at a well-defined density, providing clear evidence that this is a transition to a new phase at low densities. The next challenge is to determine the nature of this phase.

We gratefully acknowledge discussions with B. L. Gallagher, S. A. Kivelson, and C. J. Mellor and technical help from Y. Zhao. This work was supported by DOE Grant No. DE-FG02-84ER45153, BSF Grant No. 2006375, RFBR, RAS, and the Russian Ministry of Sciences.

[1] L. D. Landau, Sov. Phys. JETP **3**, 920 (1957).
[2] E. Wigner, Phys. Rev. **46**, 1002 (1934).
[3] E. C. Stoner, Rep. Prog. Phys. **11**, 43 (1947).
[4] A. V. Chaplik, Sov. Phys. JETP **35**, 395 (1972).
[5] B. Tanatar and D. M. Ceperley, Phys. Rev. B **39**, 5005 (1989).
[6] C. Attaccalite, S. Moroni, P. Gori-Giorgi, and G. B. Bachelet, Phys. Rev. Lett. **88**, 256601 (2002).
[7] R. Heemskerk and T. M. Klapwijk, Phys. Rev. B **58**, R1754 (1998).
[8] R. Fletcher, V. M. Pudalov, A. D. B. Radcliffe, and C. Possanzini, Semicond. Sci. Technol. **16**, 386 (2001).
[9] Note that a theory for the thermopower near the Anderson transition has not been developed. Our experimental results nevertheless establish the important fact that the thermopower tends toward a divergence at an electron density n_t that is distinctly different from the density for the Anderson transition.
[10] A. A. Shashkin, S. V. Kravchenko, V. T. Dolgopolov, and T. M. Klapwijk, Phys. Rev. B **66**, 073303 (2002).
[11] V. T. Dolgopolov and A. Gold, JETP Lett. **94**, 446 (2011).
[12] A. Gold and V. T. Dolgopolov, Europhys. Lett. **96**, 27 007 (2011).
[13] R. Fletcher, V. M. Pudalov, Y. Feng, M. Tsaousidou, and P. N. Butcher, Phys. Rev. B **56**, 12 422 (1997).
[14] S. Faniel, L. Moldovan, A. Vlad, E. Tutuc, N. Bishop, S. Melinte, M. Shayegan, and V. Bayot, Phys. Rev. B **76**, 161307(R) (2007).
[15] S. Goswami, C. Siegert, M. Baenninger, M. Pepper, I. Farrer, D. A. Ritchie, and A. Ghosh, Phys. Rev. Lett. **103**, 026602 (2009).
[16] Measurements in the parallel-field configuration yield the product of the effective mass and g factor, where the increase was shown to derive from a strong increase of

the electron mass while the g factor enhancement is weak [17,18].

[17] S. V. Kravchenko and M. P. Sarachik, Rep. Prog. Phys. **67**, 1 (2004).

[18] A. A. Shashkin, Phys. Usp. **48**, 129 (2005).

[19] S. V. Kravchenko, A. A. Shashkin, D. A. Bloore, and T. M. Klapwijk, Solid State Commun. **116**, 495 (2000).

[20] M. D'Iorio, V. M. Pudalov, and S. G. Semenchinsky, Phys. Lett. A **150**, 422 (1990).

[21] V. T. Dolgopolov, JETP Lett. **76**, 377 (2002).

[22] B. Spivak, Phys. Rev. B **67**, 125205 (2003).

[23] B. Spivak and S. A. Kivelson, Phys. Rev. B **70**, 155114 (2004).

[24] V. A. Khodel, J. W. Clark, and M. V. Zverev, Phys. Rev. B **78**, 075120 (2008).

[25] S. Pankov and V. Dobrosavljević, Phys. Rev. B **77**, 085104 (2008).

[26] A. Punnoose and A. M. Finkelstein, Science **310**, 289 (2005).

[27] M. Marchi, S. De Palo, S. Moroni, and G. Senatore, Phys. Rev. B **80**, 035103 (2009).

[28] G. Fleury and X. Waintal, Phys. Rev. B **81**, 165117 (2010).